Available online at www.sciencedirect.com
SCIENCE DIRECT
Chemical Physics 325 (2006) 519–524
Chemical Physics
www.elsevier.com/locate/chemphys

Sb adsorption on Cu(110), (100), and (111) surfaces

H.Y. Xiao [a], X.T. Zu [a,b,*], X. He [a], F. Gao [c]

[a] Department of Applied Physics, University of Electronic Science and Technology of China, Chengdu, 610054, People's Republic of China
[b] International Center for Material Physics, Chinese Academy of Sciences, Shenyang 110015, People's Republic of China
[c] Pacific Northwest National Laboratory, MS K8-93, P.O. Box 999, Richland, WA 99352, USA

Received 6 November 2005; accepted 25 January 2006
Available online 14 February 2006

Abstract

The adsorption of antimony on the (110), (100) and (111) surfaces of Cu has been studied using gradient-corrected density-functional calculations. Our calculations showed that all the surfaces are active for Sb adsorption and surface alloys are formed in which Sb atoms substitute Cu atom in the outermost layer, in excellent agreement with experiments. The vacancy formation energy for (110) surface is found to be the smallest and the Sb/Cu(110)$c(2\times2)$ surface alloy turns out to be energetically the most favorable. Our results are found to agree well with the available experimental and theoretical work.

Keywords: Density-functional calculations; Antimony; Copper; Surface alloy

1. Introduction

There has been increased interest in the last few years in the properties of surface alloys and in the general characteristics of epitaxial growth of both thin semiconductor and metal films. One such system which has attracted especial attention is the case of Sb adsorption on Ag(111) surface, because Sb have a surfactant effect on the homoepitaxial growth of Ag on this surface [1–6]. Numerous investigations demonstrated that when Sb is deposited on the surface Sb atoms will substitute Ag atom in the outermost layer to produce an ordered surface alloy. Early investigations performed by Scheuch et al. [7] demonstrated that Sb can also be used a surfactant for the growth of Co on Cu(111) surface. Concerning surface structural phase formed, it was reported that the Sb/Cu(111) system appears to be extremely similar [8] and the two systems do exhibit the same type of reconstruction [3].

In recent years, the adsorption of Sb on the different faces of Cu single crystals has drawn much attention and studied extensively. The structure of the Cu(100)–$p(2\times2)$–Sb phase, formed by depositing 0.25 ML Sb on clean Cu(100) at room temperature, was determined by AlShamaileh et al. [9] using tensor LEED (low energy electron diffraction) technique. The results show that a surface alloy is formed in which Sb atoms substitute Cu atom in the outermost layer. Recently, a tensor LEED study of the $c(2\times2)$–Sb adsorption structure on Cu(110) has been performed by Pussi et al. [10], who observed that the behavior of Sb adsorption on Cu(110) is similar to the Sb/Cu(100) system under same experimental conditions and the favored structure is also a substitutional surface alloy where every other top layer copper atom has been replaced by an antimony atom. Sb adsorption on Cu(111) surface has been studied with a variety of experimental techniques. A study by AES (auger electron spectroscopy)–LEED technique of dissolution and segregation of kinetics of Sb/Cu(111) with a $p(\sqrt{3}\times\sqrt{3})R30^\circ$ superstructure has been reported by Giordano and Aufray [11]. Meunier et al. have studied the atomic structure of the SbCu surface alloy at 0.33 ML by SXRD (surface X-ray diffraction) [12]. An XRD structure analysis of the $(\sqrt{3}\times\sqrt{3})R30^\circ$ reconstructions of Cu(111)–Sb surfaces was also presented by de Vries et al. [3]. MEIS (medium energy ion scattering) has been used by Bailey et al. [13] to characterize the behavior of

* Corresponding author. Tel./fax: +86 28 83201939.
E-mail address: xiaotaozu@yahoo.com (X.T. Zu).

0301-0104/$ - see front matter © 2006 Elsevier B.V. All rights reserved.
doi:10.1016/j.chemphys.2006.01.029

Cu(1 1 1) following deposition of 10 ML of Sb, and to determine the structure of the Cu(1 1 1) $(\sqrt{3}\times\sqrt{3})$R30°–Sb surface phase. Aufray et al. [14] employed ultrahigh vacuum STM (scanning tunneling microscope) at room temperature to study the surface segregation of Sb at a Cu(1 1 1) surface. Recently, Umezawa et al. investigated the structures of Cu(1 1 1) $(\sqrt{3}\times\sqrt{3})$R30°–Sb using ICISS (impact collision ion-scattering spectroscopy) [15]. Despite some minor differences concerning the atomic structure of Cu(1 1 1) $(\sqrt{3}\times\sqrt{3})$R30°–Sb surface phase these investigations agree that Sb atoms are in a substitutional position in the topmost surface layer.

Theoretically, few calculations of Sb on Cu surfaces have been performed. Woodruff and Robinson have conducted structural optimization calculation in the generalized gradient approximation (GGA) for Cu(1 1 1) $(\sqrt{3}\times\sqrt{3})$R30°–Sb surface phases [5]. For Sb adsorption on Cu(1 1 0) and Cu(1 0 0) surface, no theoretical information has been reported so far. In this work, we investigate antimony adsorption on the (1 1 0), (1 0 0) and (1 1 1) surfaces of Cu via periodic, self-consistent DFT–GGA calculations. Such method has been demonstrated to be used for calculating the electronic and structural property of medium-sized systems with predictive accuracy [16,17]. The preferred adsorption sites, optimized geometries, work function change and vibrational properties all have been presented and analyzed. The paper is organized as follows. In Section 2, the computational method we employed in this work are described briefly. In Section 3.1, we present the preferred binding sites, optimized geometric structures, adsorption energies, and the effects of surface relaxation for Sb on Cu(1 1 0), (1 0 0) and (1 1 1) surface at the coverage (Θ) of 0.25 ML. Section 3.2 concentrates on the vibrations of Sb on Cu surface. In Section 4, we draw some conclusions from the work.

2. Calculational method

All calculations were performed using VASP package. Ab initio total energy calculations within the DFT framework were carried out in this study. Three different faces of Cu single crystals, i.e., (1 1 0), (1 0 0) and (1 1 1), were modeled by supercell approach [18] with periodic boundary conditions. Top views of the three slabs are shown in Fig. 1. The influence of the thickness of slab and vacuum was explored in a series of test calculations, which leads to all the Cu surfaces being modeled by six Cu atomic layers slab with six equivalent layers of vacuum between any two successive metal slabs. Adsorption is allowed on only one of the two exposed surfaces, and the electrostatic potential is adjusted accordingly. For (1 1 0), (1 0 0) and (1 1 1) surface, we considered $c(2\times2)$, (2×2) and $(\sqrt{3}\times\sqrt{3})$R30° unit cell with one Sb adsorbate, respectively. The adsorbate and the atoms in the top three layers were allowed to relax while the atoms in the bottom three layers were fixed at the bulk truncated positions. The electron–ion interactions are described using ultrasoft pseudopotentials (USPP) [19,20] which allow us to use a cut-off energy of 350 eV for the plane-wave basis set. Both GGA-PW91 [21,22] and LDA-PZ [23] functional are used. The electronic ground state is calculated with the residuum-minimization techniques. The geometric structure is optimized with the conjugated-gradient technique. A Monkhorst–Pack mesh with $6\times6\times1$ K-point sampling within the surface Brillouin zone was used. The calculated lattice constant for bulk copper, 3.64 Å, is within 1% of the experimental value of 3.61 Å. This calculated lattice constant was used in all subsequent calculations.

3. Results and discussions

3.1. Clean surfaces

The geometries of the Cu surfaces have been studied in detail experimentally and theoretically [24–33]. In this work, we first investigated the relaxation effects of the clean Cu(1 1 0), (1 0 0) and (1 1 1) surface. The calculated results are summarized in Table 1 along with comparison of other experimental and theoretical results. For clean Cu(1 1 0) surface, the experimental results predicted a contraction for d_{12} of about −9.5% and an expansion for d_{23} of about 2% [24,26]. Our calculations yield a −8.8% inward relaxation of the first layer and 5.3% outward relaxation of the second layer, agreeing well with experiments. For Cu(1 0 0) and Cu(1 1 1) surfaces, we found that relaxation effects are almost negligible, as can be seen from Table 1. Our results are found to be comparable to most of the experimental and theoretical work [25,27–33]. It was also found that our calculations generally overestimate surface buckling. This phenomenon may be caused by the use of GGA method, which sometimes overcorrects the effects of coupling between the valence and core electrons [34–36].

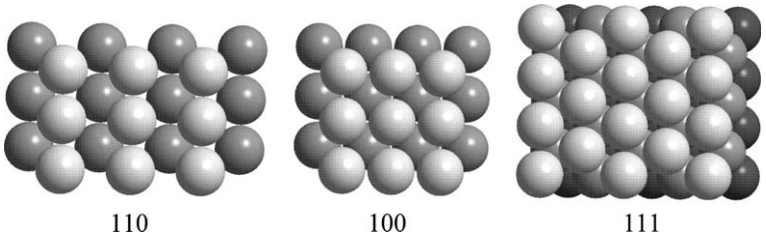

Fig. 1. Top view of the (1 1 0), (1 0 0) and (1 1 1) surfaces of Cu.

Table 1
Relaxation of the clean (1 1 0), (1 0 0) and (1 1 1) surfaces[a]

	Present study	Experiment		Theory	
	Value	Value	Ref.	Value	Ref.
1 1 0					
$\Delta d_{12}/d_0$(%)	−8.8	−10.0	[24]	−7.76	[25]
		−8.5 ± 0.6	[26]	−9.3	[27]
				−8.93	[28]
$\Delta d_{23}/d_0$(%)	5.3	1.9	[24]	4.17	[25]
		2.3 ± 0.8	[26]	2.8	[27]
				4.41	[28]
1 0 0					
$\Delta d_{12}/d_0$(%)	−2.8	−1.2	[29]	−1.06	[25]
		−2.1	[30]	−3.0	[27]
				−0.83	[28]
$\Delta d_{23}/d_0$(%)	1.0	0.9	[29]	−0.65	[25]
		0.45	[30]	0.1	[27]
				0.04	[28]
1 1 1					
$\Delta d_{12}/d_0$(%)	−0.7	0.5–1	[31]	0.56	[25]
		−0.3 ± 1.0	[32]	−1.3	[27]
		−0.7 ± 0.5	[33]	0.14	[28]
$\Delta d_{23}/d_0$(%)	0.0	0.0	[31]	−0.07	[25]
		0.0	[32]	0.6	[27]
		0.0	[33]	−0.01	[28]

[a] d_{ij}: the vertical spacing between the ith and jth atomic layer; d_0: the ideal interlayer spacing, which is 1.29, 1.82 and 2.1 Å for Cu(1 1 0), (1 0 0) and (1 1 1) surfaces, respectively.

3.2. Sb adsorption on Cu(1 1 0) surface

For Sb/Cu(1 1 0)$c(2\times2)$ system, we considered five different models: four high symmetry overlayer structures where Sb atoms occupy fourfold hollow sites, long bridge sites, short bridge sites or top sites and a surface alloy model, where Sb atoms substitute one top layer Cu atoms (see Fig. 2). The geometries of adsorption systems have been optimized and the adsorption energies have been calculated. To compare the stability of the surface-substitutional adsorption with that of the "normal" adsorption it is necessary to define the adsorption energy per adatom [37]. For the simple overlayer structures it is defined as

$$E_{\mathrm{ad}} = E_{\mathrm{Sb/Cu\text{-}slab}} - (E_{\mathrm{Cu\text{-}slab}} + E_{\mathrm{Sb\text{-}atom}}),$$

where $E_{\mathrm{Sb/Cu\text{-}slab}}$ and $E_{\mathrm{Cu\text{-}slab}}$ are the total energy of the Cu slab with or without adsorbed atoms, $E_{\mathrm{Sb\text{-}atom}}$ is the total energy of an isolated Sb atom. For the surface-substitutional site the adsorption energy was calculated by the formula

$$E_{\mathrm{ad}}^{\mathrm{sub}} = E_{\mathrm{Sb/Cu\text{-}slab}}^{\mathrm{sub}} - (E^{\mathrm{vac}} + E_{\mathrm{Sb\text{-}atom}}) + E_{\mathrm{f}}^{\mathrm{vac}}$$

and

$$E_{\mathrm{f}}^{\mathrm{vac}} = E^{\mathrm{vac}} + (E^{\mathrm{Cu\text{-}atom}} - E_{\mathrm{coh}}) - E_{\mathrm{Cu\text{-}slab}}.$$

Here, E^{vac} is the total energy per unit cell of the surface-vacancy structure, $E^{\mathrm{Cu\text{-}atom}}$ is the total energy of a free Cu atom, and E_{coh} is the Cu cohesive energy. $E_{\mathrm{Cu\text{-}slab}}$ is the total energy of the clean slab. In this work, the Cu cohesive energy was determined to be 3.62 eV from our calculations, agreeing well with experimental value of 3.54 eV [38]. Another calculation [39] within the second-moment approximation of the tight-binding theory yields a value of 4.65 eV. The surface vacancy formation energy $E_{\mathrm{f}}^{\mathrm{vac}}$ based on Cu(1 1 0)$c(2\times2)$ model was determined to be 0.25 eV.

Table 2 lists the main energetic and structural properties for Sb atoms adsorption at stable adsorption sites on Cu(1 1 0)$c(2\times2)$ surface. We found that on Cu(1 1 0) surface Sb substitutes Cu atom in the outermost layer and produces a surface alloy. The substitutional site was found to be 100 meV lower in energy than the next stable hollow sites. Using quantitative LEED, Pussi et al. [10] also observed that the favored structure is a substitutional surface alloy where every other top layer copper atom has been replaced by an antimony atom, in excellent agreements with our work. Structural analysis showed that Sb atom was rippled outward from the surface by 0.37 Å, corresponding to experimental value of 0.25 ± 0.05 Å reported by Pussi et al. [10]. Our calculated Sb–Cu bond length and interlayer spacing were also shown to be comparable to the experiments. Relaxation effect was found to be almost negligible when Sb atoms occupy substitutional

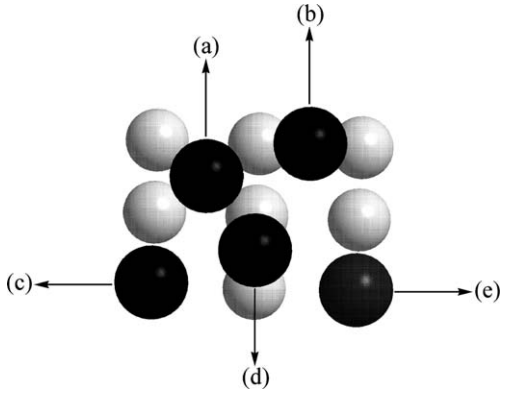

Fig. 2. Schematic plane view of the different adsorption sites for Sb adsorption on Cu(1 1 0) surface: (a) hollow site; (b) long bridge site; (c) top site; (d) short bridge site; (e) substitutional site.

Table 2
Main energetic and structural properties for Sb atoms adsorption on Cu(1 1 0)$c(2\times2)$ surface[a]

Site	E_{ads} (eV)	$d_{\mathrm{Sb–Cu}}$ (Å)	$\Delta Z_{\mathrm{Sb–Cu1}}$ (Å)	$\Delta Z_{\mathrm{Cu1–Cu2}}$ (Å)	$\Delta Z_{\mathrm{Cu2–Cu3}}$ (Å)
Clean				1.14	1.35
Hollow	−3.93	2.66	1.43	1.20	1.27
Long bridge	−3.63	2.50	1.36	1.16	1.25
Top	−2.30	2.35	1.77	0.94	1.25
Sub	−4.03	2.60	0.37	1.16	1.33
Sub[b]		2.56 ± 0.04	0.25 ± 0.05	1.25 ± 0.03	1.30 ± 0.03

[a] E_{ads}: adsorption energy. $d_{\mathrm{Sb–Cu}}$: Sb–Cu bond length; $\Delta Z_{\mathrm{Sb–Cu1}}$: the vertical separation between Sb atom and on-topmost Cu substrate; $\Delta Z_{\mathrm{Cu1–Cu2}}$: the vertical distance between the first and the second Cu layer; $\Delta Z_{\mathrm{Cu2–Cu3}}$: the vertical distance between the second and the third Cu layer. sub: substitutional sites.

[b] Ref. [10].

sites, indicating that Sb substitution has significant effect on the structure of Cu(1 1 0) surface.

3.3. Sb adsorption on Cu(1 0 0) surface

When Sb was adsorbed on Cu(1 0 0) surface, four high symmetry adsorption sites, i.e., fourfold hollow, bridge, top and substitutional sites, were considered (as shown in Fig. 3). For Cu(1 0 0)(2 × 2) surface the surface vacancy formation energy E_f^{vac} was calculated to be 0.43 eV, which is 0.18 eV larger than that of Cu(1 1 0)(2 × 2) model. The adsorption energies of Sb at different adsorption sites are presented in Table 3. It was found that top site adsorption is unfavorable and the most stable adsorption site is substitutional site, followed in decreasing order of stability by the fourfold hollow site, with the bridge site being the least stable. The energy difference between substitutional and hollow sites is found to be 0.23 eV. This finding agrees well with the LEED studies performed by AlShamaileh et al. [9], who found that despite the large size mismatch between Sb and Cu, a surface alloy is formed in which Sb atoms substitute Cu atom in the outermost layer.

The main structural parameters obtained for Sb/Cu(1 0 0)(2 × 2) system are also listed in Table 3. We found the antimony atoms are bulked toward the solid vacuum interface by 0.62 Å with respect to the first copper layer, in excellent agreement with the experimental value of 0.56 ± 0.05 Å [9]. One can see from Table 3 that the Sb–Cu bond length and the interlayer spacings obtained from our calculations also agree well with experiments. The first Cu layer was found to be contracted by −3.8% with respect to the ideal interlayer spacing, corresponding to the contraction value of −2.8% obtained for clean Cu(1 0 0) surfaces. It is clear that the structure of Cu(1 0 0) surface was affected little by Sb substitution, different from the case of Sb on Cu(1 1 0) surface.

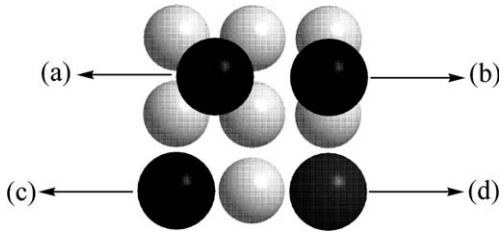

Fig. 3. Schematic plane view of the different adsorption sites for Sb adsorption on Cu(1 0 0) surface: (a) hollow site; (b) bridge site; (c) top site; (d) substitutional site.

Table 3
Main energetic and structural properties for Sb atoms adsorption on Cu(1 0 0)(2 × 2) surface

Site	E_{ads} (eV)	$d_{Sb–Cu}$ (Å)	$\Delta Z_{Sb–Cu1}$ (Å)	$\Delta Z_{Cu1–Cu2}$ (Å)	$\Delta Z_{Cu2–Cu3}$ (Å)
Clean				1.77	1.84
Bridge	−2.91	2.46	1.84	1.73	1.81
Hollow	−3.53	2.57	1.78	1.82	1.83
Sub	−3.76	2.65	0.62	1.75	1.81
Sub[a]		2.61 ± 0.05	0.56 ± 0.05	1.84 ± 0.05	1.80 ± 0.05

[a] Ref. [9].

3.4. Sb adsorption on Cu(1 1 1) surface

Optimized geometries and adsorption energies for Sb adsorption on Cu(1 1 1) surface at three distinct high symmetry sites, namely fcc hollow, hcp hollow and substitutional sites (see Fig. 4), are presented in Table 4. Experimentally [3,12–15] it was observed for Cu(1 1 1)($\sqrt{3} \times \sqrt{3}$)R30°–Sb system that the Sb atom substitutes one of the Cu atoms in the outermost layer to form a single layer surface alloy phases and the top layer is laterally displaced on the surface as in a stacking fault so that all its atoms reside at hcp hollow sites relative to the underlying Cu(1 1 1) surface. Using DFT method Woodruff and Robinson [5] found that for ($\sqrt{3} \times \sqrt{3}$)R30° periodicity this stacking-faulted configuration is indeed marginally 11 meV stable than an unfaulted configuration, and obtained structural parameters were in excellent agreements with the experimental values obtained by MEIS and ICISS [13,15]. Vries et al. [3] reported that at

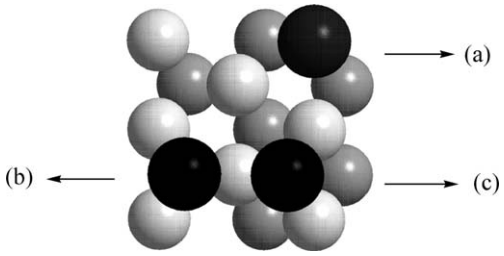

Fig. 4. Schematic plane view of the different adsorption sites for Sb adsorption on Cu(1 1 1) surface: (a) substitutional site; (b) hcp hollow site; (c) fcc hollow site.

Table 4
Main energetic and structural properties for Sb atoms adsorption on Cu(1 1 1) ($\sqrt{3} \times \sqrt{3}$)R30° surface

Site	E_{ads} (eV)	$d_{Sb–Cu}$ (Å)	$\Delta Z_{Sb–Cu1}$ (Å)	$\Delta Z_{Cu1–Cu2}$ (Å)	$\Delta Z_{Cu2–Cu3}$ (Å)
Clean				2.08	2.10
fcc hollow	−3.03	2.50	2.00	2.07	2.07
hcp hollow	−3.01	2.51	2.01	2.07	2.08
Unfaulted alloy	−3.63	2.63	0.53	2.07	2.09
Exp.[a]			0.72		
Theor.[b]	−3.840				
Faulted alloy	−3.639	2.62	0.51	2.08	2.08
Exp.[c]		2.63	0.60	1.98	2.08
Exp.[d]			0.32 ± 0.02		
Exp.[a]			0.47	2.05	2.08
Exp.[e]			0.40		
Theor.[b]	−3.851		0.47	2.09	2.07

[a] MEIS results for Cu(1 1 1)($\sqrt{3} \times \sqrt{3}$)R30°–Sb, see Ref. [13].
[b] Theoretical values for Cu(1 1 1)($\sqrt{3} \times \sqrt{3}$)R30°–Sb, see Ref. [5].
[c] SXRD results for Cu(1 1 1)($\sqrt{3} \times \sqrt{3}$)R30°–Sb, see Ref. [3].
[d] SXRD results for Cu(1 1 1)($\sqrt{3} \times \sqrt{3}$)R30°–Sb, see Ref. [12].
[e] ICISS results for Cu(1 1 1)($\sqrt{3} \times \sqrt{3}$)R30°–Sb, see Ref. [15].

$\Theta = 0.33$ ML the top layer atoms reside at hcp hollow sites relative to the underlying Cu(1 1 1) surface, while for coverages below 1/3 ML, the Sb atoms are embedded randomly at fcc positions in the top surface layer. The STM study of the earlier stages of Sb adsorption on Ag(1 1 1) of van der Vegt et al. [40] also indicated that some Sb atoms are randomly distributed in substitutional fcc sites, whereas others form islands with $(\sqrt{3}\times\sqrt{3})$R30° periodicity. Since experimentally there was no indication of ordered (2×2) phase, in this work we considered $(\sqrt{3}\times\sqrt{3})$R30° unit cell for Cu(1 1 1) surface.

The surface vacancy formation energy E_f^{vac} based on Cu(1 1 1)$(\sqrt{3}\times\sqrt{3})$R30° model was calculated to be 0.71 eV, comparing with another theoretical value of 0.92 eV [41] obtained from DFT–LDA calculations. This value was found to be much larger than that of Cu(1 1 0)$c(2\times2)$ and Cu(1 0 0)(2×2) model. Similar to the case of Sb adsorption on Cu(1 1 0) and Cu(1 0 0) surface, a preference for the substitutional site was also observed for Sb on Cu(1 1 1) surface. We found at the coverage of 0.33 ML stacking fault model is only 9 meV stable than the unfaulted alloy structure, i.e., all top layer atoms occupy hcp hollow sites relative to the underlying Cu(1 1 1) surface. In order to investigate the effects of number of surface layers on computational accuracy, the Cu(1 1 1) surfaces are also described by eight Cu layers for comparison. In this case the energy difference has been affected little by the slab layers. The finding that faulted alloy model structures are slightly stable than unfaulted alloy model agrees well with the available experimental and theoretical results [5,12,13,15].

The main structural parameters obtained for Sb/Cu-(1 1 1)$(\sqrt{3}\times\sqrt{3})$R30° system are also presented in Table 4. We found the antimony atoms are displaced outward 0.51 Å with respect to the first layer Cu atoms. This value was found to be comparable to experimental [12,13,15] and theoretical results [5]. The Sb–Cu bond length and the interlayer spacings obtained from our calculations were also shown to be in good agreements with theoretical and experimental value. A contraction of the two outer interlayer spacings with respect to the bulk value d_0 by $\Delta d_{12}/d_0 = -0.9\%$ and $\Delta d_{23}/d_0 = -0.9\%$ is obtained. Comparing with the value of $\Delta d_{12}/d_0 = -0.7\%$ and $\Delta d_{23}/d_0 = -0.0\%$, we found Sb substitution has little effect on the structure of Cu(1 1 1) surface, similar to the case of Sb on Cu(1 0 0) surface but different from the case of Sb on Cu(1 1 0) surface.

3.5. Comparison for Sb adsorption on Cu(1 1 0), (1 0 0) and (1 1 1) surface

Our calculations have shown that all the surfaces are active for Sb adsorption and in all cases the favored structures are substitutional surface alloy where every other top layer copper atom was replaced by an antimony atom. In Table 5 the most important results for Sb–Cu surface alloy on Cu(1 1 0), (1 0 0) and (1 1 1) surfaces are compared. As can be seen from Table 5, the vacancy formation energy for (1 1 0) surface is smallest and Sb/Cu(1 1 0)$c(2\times2)$ surface alloy is 0.18 and 0.46 eV more stable than Sb/Cu(1 0 0)(2×2) and Sb/Cu(1 1 1)$(\sqrt{3}\times\sqrt{3})$R30° surface alloy, respectively. Obviously the Sb/Cu(1 1 0)$c(2\times2)$ surface alloy is energetically the most favorable. It is noticeable that for Cu(1 1 0), (1 0 0) and (1 1 1) surfaces the Sb–Cu bond lengths of surface alloy are almost the same and determined to be about 2.62 Å, from which an effective antimony radius of 1.33 Å was deduced, comparable to the atomic radius of 1.45 Å [9]. To further investigate the interaction between Sb adsorbate and Cu substrate, we performed density of state (DOS) analysis for adsorption systems studied above. The DOS curves are shown in Fig. 5. Fig. 5(a) and (b) represents the DOS at the antimony atoms

Table 5
Comparison of the results for Sb adsorption on Cu substrate in the most stable structures

	E_{ads} (eV)	d_{Sb-Cu} (Å)	ΔZ_{Sb-Cu1} (Å)	$\Delta Z_{Cu1-Cu2}$ (Å)	E_f^{vac} (eV)
1 1 0	−4.03	2.60	0.37	1.16	0.25
1 0 0	−3.76	2.65	0.62	1.75	0.43
1 1 1	−3.72	2.62	0.51	2.08	0.71

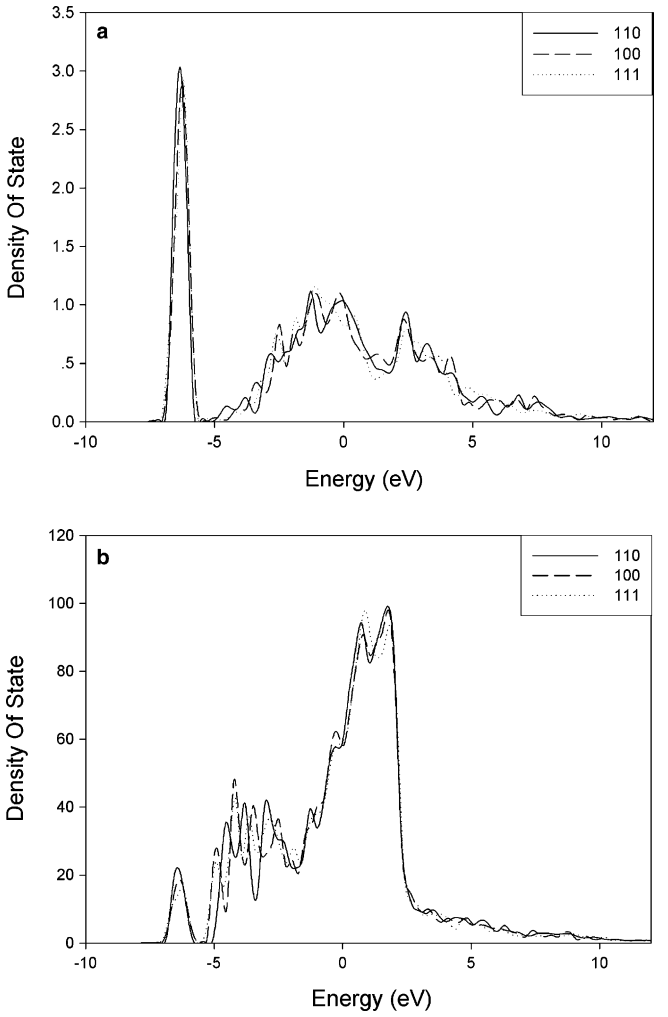

Fig. 5. DOS curves for Sb/Cu adsorption system: (a) at antimony atoms; (b) at copper atoms.

and copper atoms, respectively. The Fermi level of the adsorption system is set to 0 eV. The lowest energy peak of Sb on Cu(1 1 0) surface in Fig. 5(a), which represents 5S-derived states, is shifted downwards slightly in energy relative to that of Sb on Cu(1 0 0) and (1 1 1) surfaces, indicating that the interaction between Sb adsorbate and Cu(1 1 0) substrate is the strongest. The region from ~ -5 eV up to 5 eV consists of quantum states which contain relatively weaker 5p character. From Fig. 5(b) One can see that the Fermi energy is in a regime with a significant contribution from Cu 3d bands, so that the overlayer is clearly metallic [42].

4. Conclusions

Density functional theory with generalized gradient approximation has been used to study antimony adsorption on Cu(1 1 0), (1 0 0) and (1 1 1) surfaces. It was found that in all cases substitutional adsorption sites are preferred over other sites and surface alloys are formed, which is in perfect agreements with experiments. The vacancy formation energy has been determined to be 0.25, 0.43 and 0.71 eV for (1 1 0), (1 0 0) and (1 1 1) surfaces, respectively. Our calculations showed that Sb/Cu(1 1 0)$c(2\times 2)$ surface alloy is 0.18 and 0.46 eV more stable than Sb/Cu(1 0 0)(2×2) and Sb/Cu(1 1 1)$(\sqrt{3}\times\sqrt{3})$R30° surface alloy, respectively, suggesting that Sb/Cu(1 1 0)$c(2\times 2)$ surface alloy is energetically the most favorable. DOS analysis also showed that the interaction between Sb adsorbate and Cu(1 1 0) substrate is the strongest.

Acknowledgements

This study was supported financially by the Program for New Century Excellent Talents in University (NCET-04-0899) and the Ph.D. Funding Support Program of Education Ministry of China (20050614013) and the NSAF Joint Foundation of China (10376006) and by the Sichuan Young Scientists Foundation (03ZQ026-059).

References

[1] S. Oppo, V. Fiorentini, M. Scheffler, Phys. Rev. Lett. 71 (1993) 2437.
[2] T.C.Q. Noakes, D.A. Hutt, C.F. McConville, D.P. Woodruff, Surf. Sci. 372 (1997) 117.
[3] S.A.de. Vries, W.J. Huisman, P. Goedtkindt, M.J. Zwanenburg, S.L. Bennett, I.K. Robinson, E. Vlieg, Surf. Sci. 414 (1998) 159.
[4] E.A. Soares, C. Bitencourt, V.B. Nascimento, V.E.d. Carvalho, C.M.C.d. Castilho, C.F. McConville, A.V.d. Carvalho, D.P. Woodruff, Phys. Rev. B 61 (2000) 13983.
[5] D.P. Woodruff, J. Robinson, J. Phys.: Condens. Matter 12 (2000) 7699.
[6] P.D. Quinn, D. Brown, D.P. Woodruff, P. Bailey, T.C.Q. Noakes, Surf. Sci. 511 (2002) 43.
[7] V. Scheuch, K. Potthast, B. Voigtlander, H.P. Bonzel, Surf. Sci. 318 (1994) 115.
[8] H. Giordano, B. Aufray, Surf. Sci. 307 (1994) 816.
[9] E. AlShamaileh, K. Pussi, T. McEvoy, M. Lindroos, G. Hughes, A.A. Cafolla, Surf. Sci. 566 (2004) 52.
[10] K. Pussi, E. AlShamaileh, A.A. Cafolla, M. Lindroos, Surf. Sci. 583 (2005) 151.
[11] H. Giordano, B. Aufray, Surf. Sci. 352 (1996) 280.
[12] I. Meunier, J.-M. Gay, L. Lapena, B. Aufray, H. Oughaddou, E. Landemark, G. Falkenberg, L. Lottermoser, R.L. Johnson, Surf. Sci. 422 (1999) 42.
[13] P. Bailey, T.C.Q. Noakes, D.P. Woodruff, Surf. Sci. 426 (1999) 358.
[14] B. Aufray, H. Giordano, D.N. Seidman, Surf. Sci. 447 (2000) 180.
[15] K. Umezawa, H. Takaoka, S. Hirayama, S. Nakanishi, W.M. Gibson, Curr. Appl. Phys. 3 (2003) 71.
[16] H.Y. Xiao, X.T. Zu, Y.F. Zhang, L. Yang, J. Chem. Phys. 122 (2005) 174704.
[17] L. Xu, H.Y. Xiao, X.T. Zu, Chem. Phys. 315 (2005) 155.
[18] M.C. Payne, M.P. Teter, D.C. Allan, T.A. Arias, Rev. Mod. Phys. 64 (1992) 1045.
[19] D. Vanderbilt, Phys. Rev. B 41 (1990) 7892.
[20] G. Kresse, J. Hafner, J. Phys.: Condens. Matter 6 (1994) 8245.
[21] J.P. Perdew, K. Burke, Int. J. Quantum Chem. 57 (1996) 309.
[22] J.P. Perdew, J.P. Chevary, S.H. Vosko, K.A. Jackson, M.R. Pederson, D.J. Singh, C. Fiolhais, Phys. Rev. B 46 (1992) 6671.
[23] J.P. Perdew, A. Zunger, Phys. Rev. B 23 (1981) 5048.
[24] H.L. Davis, J.R. Noonan, Surf. Sci. 126 (1983) 245.
[25] J.C. Zheng, H.Q. Wang, A.T.S. Wee, C.H.A. Huan, Surf. Rev. Lett. 8 (2001) 541.
[26] D.L. Adams, H.B. Nielsen, J.N. Andersen, Surf. Sci. 128 (1983) 294.
[27] K.P. Bohnen, K.M. Ho, Surf. Sci. Rep. 19 (1993) 99.
[28] J. Wan, Y.L. Fan, D.W. Gong, S.G. Shen, X.Q. Fan, Model. Simul. Mater. Sci. Eng. 7 (1999) 168.
[29] D.M. Lind, F.B. Dunning, G.K. Walter, H.L. Davis, Phys. Rev. B 35 (1987) 9037.
[30] R. Mayer, C. Zhang, K.G. Lynn, W.E. Frieze, F. Jona, P.M. Marcus, Phys. Rev. B 35 (1987) 3102.
[31] I. Bartos, A. Barbievi, M.A.V. Hove, W.F. Chung, Q. Cai, M.S. Altman, Phys. Rev. B 2 (1995) 477.
[32] S.P. Tear, K. Roll, M. Prutton, J. Phys. C 14 (1981) 3297.
[33] S.A. Lindgren, L. Wallden, J. Rundgren, P. Westrin, Phys. Rev. B 29 (1984) 576.
[34] G. Kresse, J. Furthmüller, J. Hafner, Phys. Rev. B 50 (1994) 13181.
[35] F. Favota, A.D. Corso, A. Baldereschi, J. Chem. Phys. 114 (2001) 483.
[36] Y. Juan, E. Kaxiras, R.G. Gordon, Phys. Rev. B 51 (1995) 9521.
[37] J. Neugebauer, M. Scheffler, Phys. Rev. B 46 (1992) 16067.
[38] C. Kittel, Introduction to Solid State Physics, Wiely, New York, 1966.
[39] N.I. Papanicolaou, G.C. Kallinteris, G.A. Evangelakis, D.A. Papaconstantopoulos, M.J. Mehl, J. Phys.: Condens. Matter 10 (1998) 10979.
[40] H.A.v.d. Vegt, J. Vrijmoeth, R.J. Behm, E. Vlieg, Phys. Rev. B 57 (1998) 4127.
[41] H.M. Polatoglou, M. Methfessel, M. Scheffler, Phys. Rev. B 48 (1993) 1877.
[42] K. Doll, Phys. Rev. B 66 (2002) 155421.